

Millimetric ground-based observations of Cosmic Microwave Background Anisotropy

L. Piccirillo¹, B. Femenía², N. Kachwala¹, R. Rebolo², M. Limon¹, C.M. Gutiérrez²,
J. Nicholas¹, R. K. Schaefer¹ and R.A. Watson^{2,3}

Received _____; accepted _____

arXiv:astro-ph/9609186v4 4 Dec 1996

¹Bartol Research Institute, University of Delaware, Newark, DE 19716

²Instituto de Astrofísica de Canarias, 38200 La Laguna, Spain

³University of Manchester, Nuffield Radio Astronomy Laboratories, Jodrell Bank,
Macclesfield, Cheshire, SK11 9DL, UK

ABSTRACT

First results of a Cosmic Microwave Background (CMB) anisotropy experiment conducted at the Observatorio del Teide (Tenerife, Spain) are presented. The instrument is a four channel (3.1, 2.1, 1.3 and 1.1 mm) ^3He bolometer system coupled to a 45 cm diameter telescope. The resultant configuration is sensitive to structures on angular scales $\sim 1^\circ - 2^\circ$. We use the channels at the two highest frequencies for monitoring the atmosphere, and apply a simple method to subtract this contribution in channels 1 (3.1 mm) and 2 (2.1 mm). The most intense structure at these two frequencies is the Galactic crossing with peak amplitudes of $\sim 350 \mu\text{K}$. These crossings have been clearly detected with the amplitude and shape predicted. This demonstrates that our multifrequency observations allow an effective assessment and subtraction of the atmospheric contribution. In the section of data at high Galactic latitude we obtain sensitivities $\sim 40 \mu\text{K}$ per beam. The statistical analyses show the presence of common signals between channels 1 and 2. Assuming a simple Gaussian auto-correlation model with a scale of coherence $\theta_c = 1.32^\circ$ for the signal, a likelihood analysis of this section of data reveals the presence of fluctuations with intrinsic amplitude $C_0^{1/2} = 76_{-32}^{+43} \mu\text{K}$ (68 % CL including a $\sim 20\%$ calibration uncertainty). Since residual atmospheric noise might still contaminate our results, we also give our result as an upper limit of $118 \mu\text{K}$ at 95% c.l.

Subject headings: Cosmology: cosmic microwave background - Observations

1. INTRODUCTION

Measurements of fluctuations in the Cosmic Microwave Background (CMB) radiation provide one of the most direct tests of theories for the formation of structure in the universe. On large angular scales where the fluctuations are produced by the Sachs-Wolfe effect in the last scattering surface, the overall normalization $Q_{rms-PS} \sim 18 \mu\text{K}$ is well established by the COBE DMR (Bennett et al. 1996) and the Tenerife beam-switching (Hancock et al. 1996) experiments. On smaller scales ($\sim 1^\circ$) the acoustic effects on the last scattering surface are expected to enhance the level of fluctuations relative to those at larger angular scales, giving rise to a feature in the power spectrum of the CMB fluctuations, the so-called "Doppler peak", with a position and shape which depends on the values of cosmological parameters (the curvature of the universe, the Hubble constant and the baryonic contribution). The current observations have recently started to allow a first determination of the position and height of this peak (Netterfield et al. 1996, Scott et al. 1996). Nevertheless more observations are needed to reduce uncertainties due to residual atmospheric signals or diffuse Galactic contamination. The main aim of the present experiment is to fill the gap in ℓ space between the IAC-Jodrell Bank beam-switching experiments (Hancock et al. 1994) with a flat spectrum weighted $\ell = 20 \pm 8$, and both the ACME South Pole (Gundersen et al. 1995) ($\ell = 68_{-32}^{+38}$) and the Saskatoon experiment (Netterfield et al. 1995). The experiment consists in a multichannel bolometer detector which is sensitive to multipoles in the range $\ell = 38 - 77$ with the maximum sensitivity at $\ell = 53$. Here we present results of our first observing campaign in the summer of 1994.

2. INSTRUMENTAL SET-UP

The instrument is described in detail elsewhere (Piccirillo 1991, Piccirillo & Calisse 1993). In summary, the optics consist of a primary off-axis parabolic mirror (45 cm

diameter) coupled to a secondary off-axis hyperbolic mirror (28 cm diameter). The detector is a four channel photometer equipped with ^3He bolometers working at 0.33K. The bands are centered at 3.3, 2.1, 1.3 and 1.1 mm wavelengths (channels 1, 2, 3 and 4) as defined by a combination of resonant mesh filters. The instrumental noise is 3, 1, 1.6 and 1.2 $\text{mK}\cdot\sqrt{\text{sec}}$ in thermodynamic units for channels 1 to 4 respectively. High frequency leaks are blocked by a combination of fluorogold, black polyethylene and Pyrex glass filters. Laboratory tests have been done to check for the absence of significant leaks in the filters. The telescope is surrounded by 45° aluminum radiation shields fixed to the ground. The beam and side-lobes have been extensively checked by placing a distant Gunn source oscillating within Channel 1 band. An accurate bi-dimensional map of the beam shape has been obtained (20° by 20°). We also studied the far field side lobe structures down to about -72 dB. These analyses show that the beam response can be approximated by a Gaussian with $\text{FWHM}=2.^\circ 4$ and that no significant side-lobes are found.

The observing strategy consists of daily drift scans done at fixed position in azimuth and elevation. The beam throw in the sky is achieved by fixing the secondary mirror and chopping sinusoidally the primary mirror, according to $\theta(t) = \theta_0$, $\phi(t) = \phi_0 + \alpha_0 \times \sin(2\pi f_w t + \psi)$ where $\phi(t)$ and $\theta(t)$ denote the azimuth and elevation respectively, $(\phi_0, \theta_0) = (0^\circ, 78.5^\circ)$ is the initial position of the antenna (see next section), $\alpha_0 = 2.6^\circ$ is the zero-to-peak azimuthal chopping amplitude at a reference frequency $f_w = 4$ Hz. The demodulation of the signal is done online in software by evaluating the amplitude of the first (4 Hz) and second (8 Hz) harmonic of the reference frequency. The resulting sky pattern for the transit of a point-like source resembles respectively the well known 2-beam and 3-beam response. In this paper we only deal with the second-harmonic demodulated data. We measured a stable DC offset (about 10 and 15 mK for, respectively, Ch1 and Ch2) which is partly due to the arc-shaped motion of the beam in the sky, i.e., the axis of rotation of the wobbling mirror is not exactly vertical, so the center position of the beam is a few arcminutes higher than

the two lateral position. The absolute pointing error has been estimated by observing the millimeter emission of the full Moon; conservatively we assumed that this error was not larger than the diameter of the Moon ($\sim 30'$). The calibration constants, for each channel, have been chosen to give 1 K signal when the central beam is completely filled with a 1 K source. The system is calibrated using cryogenic cold loads and has been checked in the field performing hot/cold load tests, raster scans of the Moon and of the Gunn source. The calibrations are consistent to about 20 % absolute accuracy.

3. OBSERVATIONS AND DATA PROCESSING

The observations were carried out at Observatorio del Teide in Tenerife (Spain) during June and July 1994. This observing site is at an altitude of 2400 m and has been shown to have extremely good atmospheric transparency and stability (Watson *et al.* , in preparation). The precipitable water vapour during the campaign was below 1.5 mm for 10 % of the time. The observed region of the sky was the strip at declination $\delta = 40^\circ$ where we collected about 550 hours of observations. This declination has been extensively measured from this site at larger angular scales ($\sim 5^\circ$) and lower frequencies (10, 15 and 33 GHz) with reported detections of structures in the CMB by the Jodrell Bank-IAC experiments (Hancock et al. 1994).

The experiment was operated only during the night to avoid contamination from solar radiation. Fluctuations in the atmospheric emission are the main source of random noise in our system. The rms of the data collected during several consecutive hours shows that the sky noise of the data binned to 10 s was of the order of 5.1, 6.8, 11.5 and 13.6 mK for channels 1, 2, 3 and 4 respectively during typical observing nights. We experienced few nights with excellent observing conditions during which the noise dropped down by a factor ~ 3.5 in all channels. Even in these cases the atmospheric noise is larger than the

instrumental noise and therefore a major goal in our processing is to assess and subtract this unwanted source of noise. We can reduce the atmospheric noise in channel 1 and 2 by subtracting the extrapolated signal from channel 4 (1.1 mm band) which is the most sensitive to atmospheric gradients. We checked also that extrapolating channel 3 (1.3 mm) produces similar results. In each channel i we have a superposition of astronomical signal and atmospheric signal: $\Delta T_{ANT,i} = \Delta T_{ANT,i}^{astro} + \Delta T_{ANT,i}^{atm}$, where all terms are expressed in antenna temperature ($T_{ANT,i}$) and $\Delta T_{ANT,i}^{atm} = \alpha_i \Delta T_{ANT,4}^{atm}$. Since the bulk of the signal in each channel is due to the atmospheric emission and the sky signal is expected to be much smaller, a linear fit of channel i versus channel 4 provides a very good estimation of α_i . For each channel we have to solve the following equation to obtain the sky signal:

$$\Delta T_{ANT,i} = \frac{f_i}{c_i} \Delta T_i^{astro} + \left(\Delta T_{ANT,4} - \frac{f_4}{c_4} \frac{1}{\rho_{i4}} \Delta T_i^{astro} \right) \times \alpha_i \quad (1)$$

where f_i and f_4 are the atmospheric transparencies at channels i and 4 computed using measurements of the water vapour content, pressure and temperature of the atmosphere (Cernicharo 1985). $\Delta T_{ANT,i}$ and $\Delta T_{ANT,4}$ are the data in channels i and 4 in antenna temperature units; ΔT_i^{astro} is the astronomical signal in thermodynamic temperature units; c_i and c_4 are the Rayleigh-Jeans to thermodynamic conversion factors: $\Delta T_{ANT,i} = \frac{1}{c_i} \Delta T_i$ ($c_i = 1.29, 1.66, 3.66, 4.82$ for channels 1 to 4 respectively) and ρ_{i4} is the fraction of the astronomical signals seen at channels i and 4: $\rho_{i4} = 1$ for CMB signal (i.e., outside the Galactic Plane crossing), $\rho_{i4} \neq 1$ in the area of the Galactic Plane crossing and evaluated according to our predictions for the Galactic foregrounds. Notice that the method requires a prior knowledge of the fraction of the signal expected in the channel i and in channel 4 (ρ_{i4}). In the case of the crossing of the Galactic Plane, we use ρ_{i4} as obtained from our estimations. However, different models in the literature yield essentially the same values for the ratios ρ_{i4} and therefore we are confident that the recovered Galactic Plane is nearly

model independent.

The atmospheric cleaning procedure was run on the data binned in 10 sec intervals, so that the noise is dominated by atmospheric noise in all channels. After cleaning, the 10 s binned scans are binned again to 4 minute bin size, so the beam is sampled with at least three points. The typical rms of these cleaned 4 minute binned scans are 0.33 and 0.29 mK for channels 1 and 2 respectively. These scans have an offset drift (always less than 0.6 mK for both channels) which we remove by fitting and subtracting combinations of sinusoidal functions with periods equal or larger than 72 degrees in RA, hence much larger than the scales at which our instrument is sensitive. We then proceed with obtaining the final data set by stacking all individual scans where the rms does not exceed 0.5 and 0.55 mK for channels 1 and 2 respectively. In this way we finally use 179 and 129 hours of data for channels 1 and 2 in order to form the final data set (33% and 23 % of the total data). The overlap in the data used in channel 1 and channel 2 amounts to 89 hours. Fig. 1 shows the results in thermodynamic temperatures obtained for channels 1 (*a* and *b*) and 2 (*c* and *d*) in the two sections of data away of the Galactic plane ($|b| \gtrsim 15^\circ$). The data have been binned in increments of 1° in RA. The visual appearance of the results of channel 1 is nearly featureless, with all the points lying below the two-sigma level while channel 2 possibly shows the presence of signal. The mean error-bar in the results of each channel is $\sim 70 \mu\text{K}$ in a 1° bin in RA. In Fig. 1*e* and 1*f* we plot the sum $((\text{Ch 1}+\text{Ch2})/2)$ and in 1*g* and 1*h* the difference $((\text{Ch 1}-\text{Ch2})/2)$ of both channels.

4. GALACTIC FOREGROUNDS

We have analyzed the Galactic contribution including the synchrotron, free-free and dust emission. The first two processes can be modeled by extrapolating the low frequency surveys at 408 MHz (Haslam et al. 1982) and 1420 MHz (Reich & Reich 1986). We use

a single power law to model the joint emission from these processes: $T_{ff-sync} \propto \nu^{-\beta}$. In the Galactic Plane crossing at RA=305° the free-free emission is expected to dominate over synchrotron due to the presence of the source Cyg A and other unresolved HII regions and therefore the spectral index is $\beta \sim 2.1$. This was additionally checked by obtaining the β values from the 1420 MHz map, which reproduce the Galactic plane crossings at Dec=+40° both in the 33 GHz Tenerife beam-switching scans (Davies et al. 1996, Gutiérrez 1992) and in the 53 and 90 GHz COBE-DMR maps. We obtain $\beta = 2.11 \pm 0.05$, which is the value that we adopted. With this value of β the free-free and synchrotron contamination is negligible at our frequencies. This is consistent with Hancock et al. 1996 which found that at 33 GHz and $\delta = 40^\circ$ this contamination is less than $8 \mu K$ on scales of about 5° . The dust contribution was estimated by using the 240 μm DIRBE map as Galactic template and extrapolated to our frequencies using the model obtained in Boulanger et al. 1996. According to this model the dust emission is well described by a grey body of emissivity $\gamma = 2$ (Reach et al. 1995) and with a dust temperature $T_d=17.5$ K: $I_\nu \propto \nu^\gamma B_\nu(T_d)$. In Fig 2 we show the prediction (dashed line) for the Galactic emission and our results for channel 1 (top) and channel 2 (bottom). The general agreement between the predictions and our measurements constitute an important check on the performance of our system and our method of subtracting the atmosphere. Any reasonable combination of γ and T_d produces a negligible dust contribution outside the area of the main Galactic Plane crossing: $rms_D(ch 1) = 0.5 \mu K$ and $rms_D(ch 2) = 1.6 \mu K$. In this paper we have ignored such contribution. A more detailed analysis will be presented in a forthcoming paper.

5. STATISTICAL ANALYSIS

We have analyzed statistically the data of channels 1 and 2 in the ranges RA₁=241° – 285° and RA₂=331° – 20° which are at Galactic latitudes $|b| \gtrsim 15^\circ$. We

computed the correlation function to check for the presence of common structures in both channels. Fig. 3 shows the most relevant results obtained. In panel *a* the cross-correlation between channels 1 and 2 is shown, in panel *b* we show the auto-correlation of the combined scan $(\text{Ch 1} + \text{Ch 2})/2$ and panel *c* shows the auto-correlation of the difference scan $(\text{Ch 1} - \text{Ch 2})/2$. The error-bars in each of the three panels represent the 68% confidence levels and have been computed using Monte Carlo techniques. Due to the experimental configuration, the expected correlation in our data, from signals on angular scales at which the instrument is sensitive, will show a characteristic pattern with a positive feature at small angles, followed by a negative bump at angles $\sim 4^\circ - 10^\circ$, and then flat at larger angles. Visual evidence of a signal with this shape exists in both *a* and *b* panels, indicating a possible correlated signal between channels. The solid lines corresponds to the expected correlation for a model estimated using a likelihood analysis (see below). This model has an intrinsic amplitude of $86 \mu\text{K}$ and a coherence angle $\theta_c = 2.1^\circ$, which corresponds to the amplitude and angle at which the maximum of the likelihood surface is attained for the combined analysis on channel 1 and 2. In *c* there is no evidence of structure, which is compatible with the expectations in the case of pure uncorrelated noise (dashed bands). Second, a likelihood analysis was used to determine the amplitude and origin of the signals. Our analysis assumed a Gaussian auto-correlation function (GACF) for the CMB signal: $C_{intr}(\theta) = C_0 \exp(-\theta^2/2\theta_c^2)$. The GACF models together with its limitations and connections to more realistic scenarios have been widely discussed in the literature (see White & Scott 1994) and we adopt it to quote preliminary results, leaving physically motivated models for a future analysis. Table 1 presents a summary of the likelihood results for the coherence angle of highest sensitivity ($\theta_c = 1.32^\circ$). Upper limits and detections are quoted at 95 % C.L. and 68 % C.L. respectively. The analysis of channel 1 does not show evidence of signal in any of the two ranges considered with a limit $C_0^{1/2} < 72 \mu\text{K}$, while for channel 2 we detect signal in both RA ranges. We made also a joint likelihood analysis

on channel 1 and 2 assuming that both channels have been measuring the same signal. This gives a detection $C_0^{1/2} = 76_{-21}^{+23} \mu\text{K}$. Including the error in the absolute calibration we obtain $C_0^{1/2} = 76_{-32}^{+43} \mu\text{K}$. Even though these results are compatible, we cannot exclude a possible frequency dependence of the detected signals. A two-dimensional (in the plane C_0 - θ_c) joint analysis of both channels shows a well defined peak at $C_0^{1/2}=86 \mu\text{K}$, $\theta_c = 2.1^\circ$; the expected correlation in our data for such a signal is plotted as the solid lines in Figs. 3a and b. The likelihood analysis shows the presence of a clear signal in channel 2, while channel 1 is compatible with noise; this indicates a source of non-CMB contaminant in channel 2. It is unlikely that the data are contaminated significantly by the Galaxy (see previous section). If we convert our results from $(C_0^{1/2}, \theta_c)$ to band power estimates, we find $\sqrt{\ell(\ell+1)C_\ell/2\pi} = 7.7_{-5.1}^{+11.3} \cdot 10^{-10}$, marginally consistent with the Standard CDM model prediction of $1.7_{-0.2}^{+0.3} \cdot 10^{-10}$ at our $\bar{\ell} = 53$ (Steinhardt 1994). The excess of signal seen in Ch2 might indicate that some residual atmospheric noise is still contaminating our results. Therefore we also quote an upper limit of $118 \mu\text{K}$ at 95% C.L. A more robust atmospheric subtraction technique together with a spectral index analysis of the measured fluctuations has been applied to our data set confirming that part of the signal seen in Ch2 is of atmospheric origin. We will report these new results in a future paper.

This work has been supported by a University of Delaware Research Foundation (UDRF) grant, by the Bartol Research Institute and spanish DGICYT project PB 92-0434-c02 at the Instituto de Astrofísica de Canarias. We want to thank L. Page and S. Meyer for considerable help in all the phases of this project. A special thank for the support of L. Shulman, J. Poirer, R. Hoyland and the technical staff of the Observatorio del Teide. Finally we would like to thank the staff from the Instituto Nacional de Meteorología at Tenerife who very kindly provided us with the atmospheric data used in this analysis.

	RA ₁	RA ₂	RA ₁ +RA ₂
Ch1	< 92	< 115	< 72
Ch2	94 ⁺⁶³ ₋₅₄	109 ⁺⁷¹ ₋₆₄	101 ⁺⁵⁰ ₋₄₈
Ch1 & Ch2	72 ⁺⁵⁰ ₋₄₅	79 ⁺⁵¹ ₋₄₅	76 ⁺⁴³ ₋₃₂

Table 1: Table 1. Likelihood results in μK CMB. A 20% calibration uncertainty has been included.

REFERENCES

- Bennett, C. L., 1996, *Ap. J.*, 464, L1
- Boulanger, F., Abergel, A., Bernard, J.-P., Burton, W.B., Désert, F.-X., Hartmann, D.,
Lagache, G. & Puget, J.-L., *Astr. Ap.* , submitted
- Cernicharo, J., 1985, IRAM Internal Report,52
- Davies, R.D., Watson, R.A., Gutiérrez, C.M., 1996, *MNRAS*, 278, 925
- De Bernardis, P., Masi, S., Vittorio, N., 1991, *ApJ*, 382, 515
- Gundersen, J. O., et al. 1995, *Ap. J.* , 443, L57
- Gutiérrez, C.M. 1992, PhD, Universidad de La Laguna
- Hancock, S., et al., 1994, *Nature*, 367, 333
- Hancock, S., et al., 1996, *MNRAS*, submitted
- Haslam et al, 1982, *A&A*,100,209
- Lineweaver, C.H. et al., 1995, *ApJ*, 448, 482
- Netterfield, C. B., Jarosik, N., Page, L., Wilkinson, & Wollack, E. J., 1995, *Ap. J.* , 445,
L69
- Netterfield, C. B., Devlin, M.J., Jarosik, N., Page, L., & Wollack, E. J., 1996, preprint
astro-ph/9601197
- Piccirillo L., 1991, *Rev. Sci. Instr.*, 62, 1293
- Piccirillo L. & Calisse P., 1993, *ApJ*, 411, 529
- Reach, W. T. et al., 1995, *ApJ*, 451, 188

Reich, P., Reich, W., 1986, A&A, 63,205

Scott, P.F., Saunders, R., Pooley, G., O’Sullivan, C., Lasenby, A.N., Jones, M., Hobson, M.P., Duffett-Smith, P.J. & Baker, J., 1996, Ap. J. , 461, L1

Steinhardt, P.J.,in Proc. CWRU Conf. on the CMB, CMB Anisotropies Two Years After COBE: Observations, Theory, and the Future, ed. L. Krauss (Singapore: World Scientific)

White, M. & Scott, D., 1994, in Proc. CWRU Conf. on the CMB, CMB Anisotropies Two Years After COBE: Observations, Theory, and the Future, ed. L. Krauss (Singapore: World Scientific)

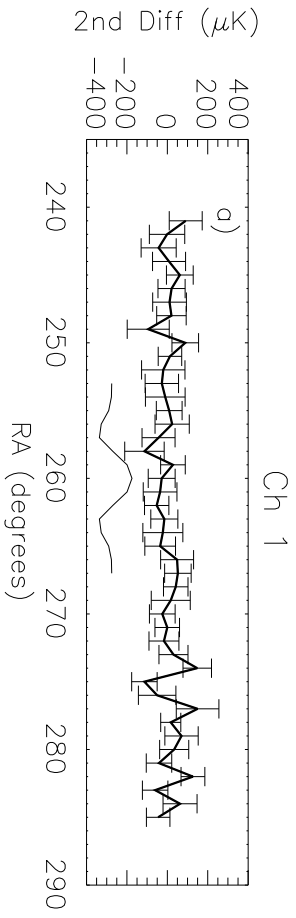
Wright et al., 1991, ApJ, 381, 200

FIGURE CAPTIONS

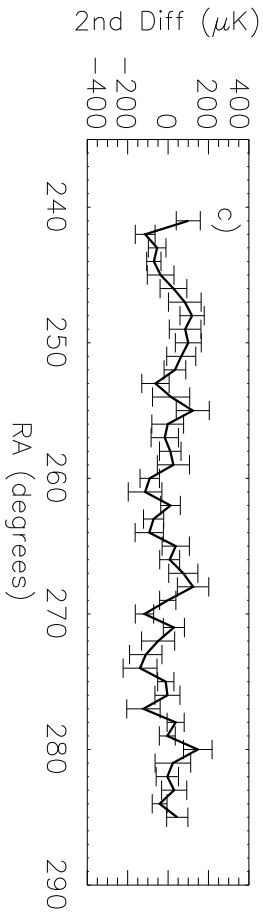
Fig. 1.— The stacked data sets at 3.3 mm (*a* and *b*), 2.1 mm (*c* and *d*), the addition (*e* and *f*) and the difference (*g* and *h*). In panel 1*a* we show the 3-beam profile indicating the instrumental response to a point source. Units refer to thermodynamic temperatures in this and following figures.

Fig. 2.— Comparison of data at the Galactic Plane crossing at $l \sim 80.2^\circ$ (solid line) and predictions of foreground emission (dashed line) for channels 1 and 2 (see main text for details).

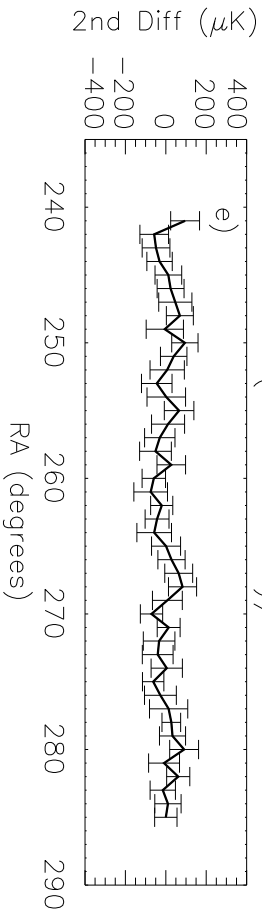
Fig. 3.— Results of the correlation analysis: (*a*) the cross-correlation of Ch 1 with Ch 2, (*b*) the auto-correlation of $(\text{Ch1} + \text{Ch2})/2$ and (*c*) the auto-correlation of $(\text{Ch1} - \text{Ch2})/2$. The solid lines in (*a*) and (*b*) is the correlation obtained with a likelihood analysis, and the dashed line in (*c*) is the 95 % C.L. for uncorrelated noise.



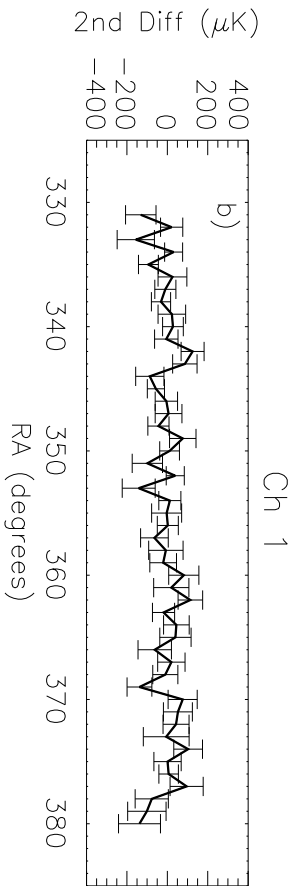
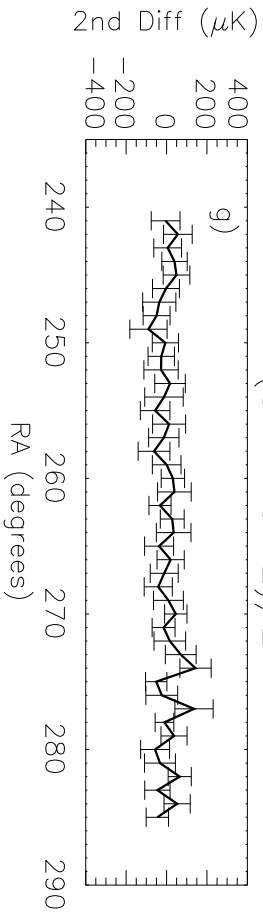
Ch 2



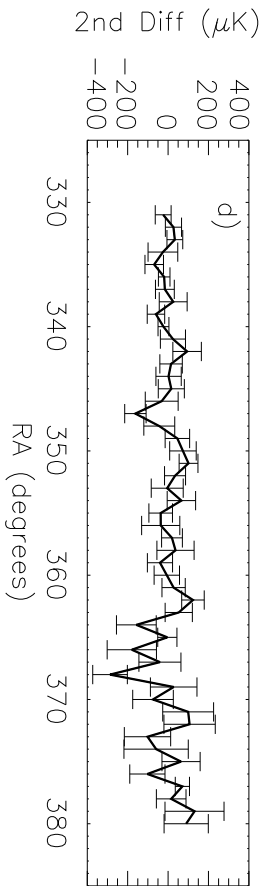
$(\text{Ch 1} + \text{Ch 2})/2$



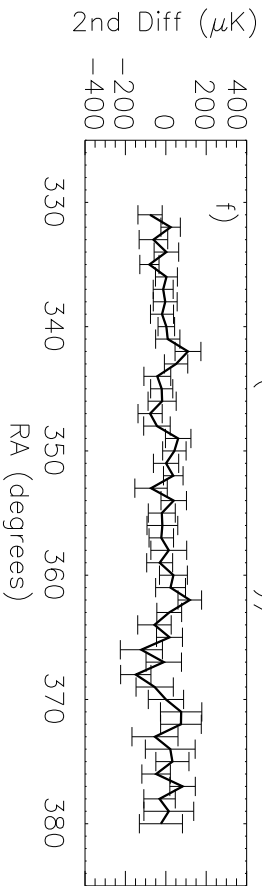
$(\text{Ch 1} - \text{Ch 2})/2$



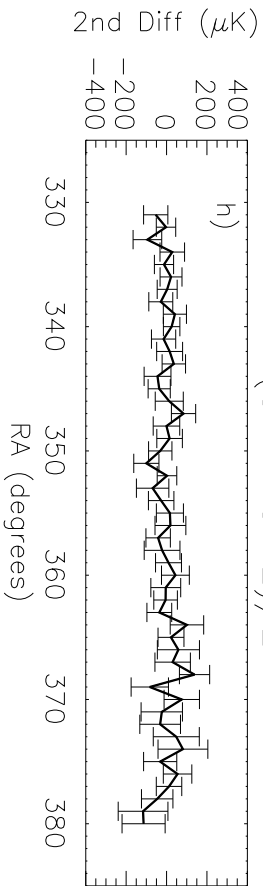
Ch 2



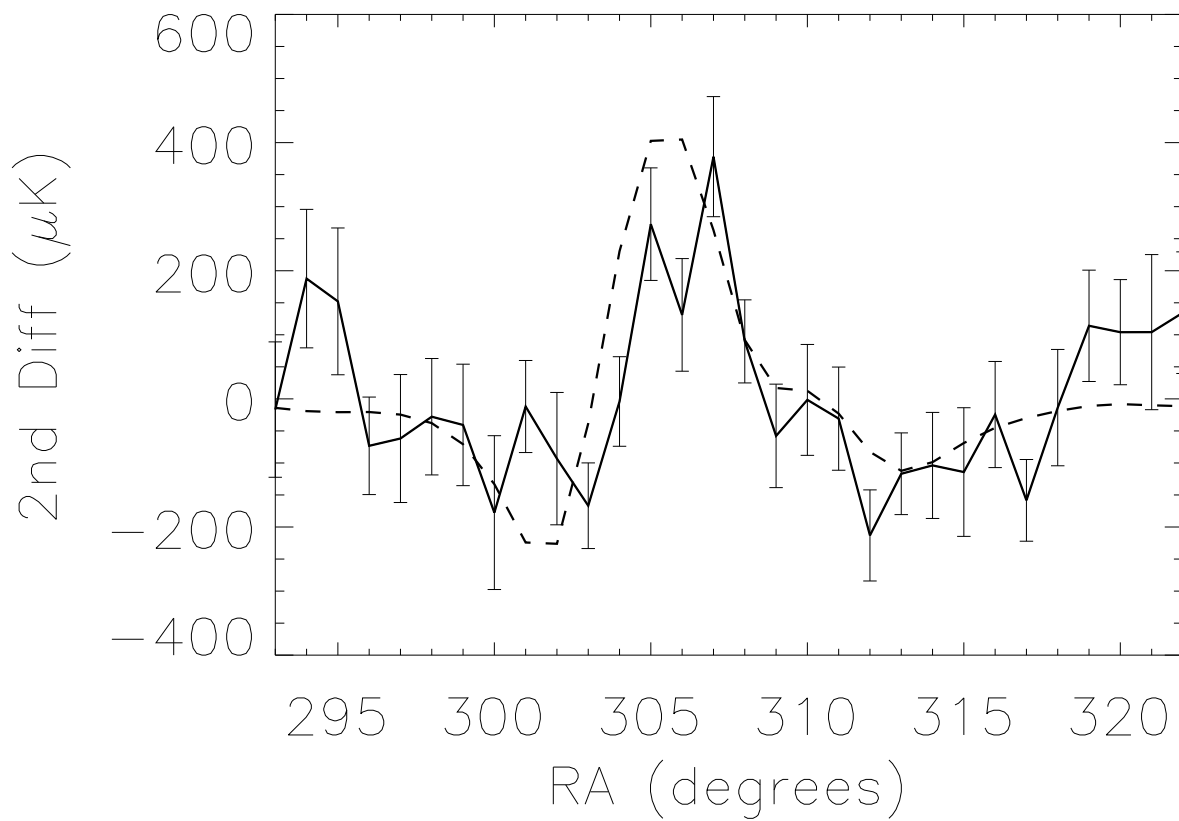
$(\text{Ch 1} + \text{Ch 2})/2$



$(\text{Ch 1} - \text{Ch 2})/2$



Ch 1



Ch 2

